Journal of Materials Chemistry A

Controlled metal loading on poly-2-acrylamido-2-methyl-propane-sulfonic acid membrane by ion-exchange process to improve electrodialytic separation performance for mono/bi-valent ions

Journal:	*Journal of Materials Chemistry A*
Manuscript ID:	TA-ART-06-2015-004468.R2
Article Type:	Paper
Date Submitted by the Author:	24-Jul-2015
Complete List of Authors:	Thakur, Amit; Central Salt and Marine Chemicals Research Institute, Electro-membrane processes Manohar, Murli; Central salt and Marine Chemicals Research Institute, Electro-membrane processes Bhavnagar, Gujarat, India, Electro-membrane processes Shahi, Vinod; Central salt and Marine Chemicals Research Institute, Electro-membrane processes

Controlled metal loading on poly(2-acrylamido-2-methyl-propane-sulfonic acid) membrane by ion-exchange process to improve electrodialytic separation performance for mono/bi-valent ions

Amit K. Thakur,[a] Murli Manohar,[a,b] Vinod K. Shahi[*a,b]

[a]*Electro-Membrane Processes Division, CSIR-Central Salt and Marine Chemicals Research Institute (CSIR-CSMCRI), Council of Scientific & Industrial Research (CSIR), Gijubhai Badheka Marg, Bhavnagar- 364 002, (Gujarat), INDIA*
Fax: +91-0278-2566970; E-mail: vkshahi@csmcri.org; vinodshahi1@yahoo.com

[b] *Academy of Scientific and Innovative Research, CSIR-Central Salt and Marine Chemicals Research Institute (CSIR-CSMCRI), Council of Scientific & Industrial Research (CSIR), Bhavnagar-364002, (Gujarat), INDIA*

Highly cross-linked poly(2-acrylamido-2-methyl-propane-sulfonic acid) (PMPS) based cation-exchange membranes (CEMs) were prepared and mono-valent selectivity of the membrane was significantly improved using pore-sieving strategy by metal (copper) loading by ion-exchange process. Prepared membranes were characterized for their morphological, physicochemical, electrochemical, and electrodialytic properties. Metal (Cu) loading in the PMPS membrane matrix improved thermal, mechanical, oxidative and hydrolytic stabilities. Results demonstrated that fine control over membrane permselectivity is possible and can be effectively tuned. Metal modification on the CEM surface improved the blocking behaviour and restricted the transport (leakage) of bi-valent metal cations (Ni^{2+}, and Zn^{2+}) during electrodialytic separation of mono- and bi-valent ions. However, partial deterioration in membrane ionic conductivity showed slight adverse effect on electrodialytic performance of the modified membrane. Extremely low Zn^{2+} leakage for prepared PMPS-3 membrane in compare with other state-of-the-art CEM was attributed to excellent pore-size sieving effect. Metal loaded PMPS-3 membrane showed improved surface compactness, which hindered easy accessibility of bulky counter-ion (Ni^{2+}/Zn^{2+}) to fixed charge and thus quite low transport (leakage) of bi-valent ions was observed.

Introduction

Membrane science and technology has received great attentions for environmental protection, waste water treatment and food/pharmacy processing.[1,2] Ion exchange membranes (IEMs) are widely used for desalination of sea water and brackish water by electrodialysis and other separation applications.[3-11] Recovery of multi-valent metal ions from the effluents of hydrometallurgy/electroplating industries is one of the important applications of electrodialysis.[12-14] Specific mono-valent selective cation-exchange membranes are essential part for all these applications. To develop specific selective IEMs, selection of functional groups and polymeric matrix, use of additives, alteration in degree of cross-linking, uniform distribution of charged groups and additives etc are vital requirements.[15-17] To improve the mono-valent permselectivity for cation-exchange membranes (CEMs), surface modification was considered as feasible route.[2,6,17,18-20]

Surface medication of CEMs involves thin layer deposition of cationic polymers (polyethylenimine, polyaniline, polypyrrole etc).[18,19, 21-25] In addition, incorporation of fillers, especially metal nanoparticles (such as titanium dioxide),[26,27] amide-acid bonding,[28-30] organic-inorganic composite mono-valent cation selective membranes,[31] etc were also considered as effective tool to improve mono-valent selectivity of CEMs. Layer-by-layer modification of CEM using poly(ethyleneimine) (PEI)/poly(styrenesulfonate) (PSS) polyelectrolyte, and annealing treatment are reported to improve the mono-valent selectivity by pore blocking.[32-34] Surface modification by polypyrrole/polyaniline formed highly rigid/tight polymer layer with weakly basic anion-exchange groups, and restricted permeation of counter-ions into the interior of the membrane. While in case of pore filled membrane, leaching out of filler is a serious problem. Furthermore, long-term stability of modified membrane surface, and resulting membranes were, however insufficient.[18] In addition, during surface modification by thin conducting polymer (polyaniline) layer, membrane

permselectivity was governed by location of polyaniline in the membrane matrix (non-homogeneous deposition).[19] Thus, some progress is still required to develop novel materials and methodology for membrane modification in a high-performance, eco-friendly and low-cost manner.

In this work we prepared cross-linked CEM based on poly(2-acrylamido-2-methyl-propane-sulfonic acid) (PMPS) and poly(vinyl alcohol) (PVA). The choice of PMPS was based on its superior ion conducting ability and functional charged nature, comparable to Nafion,[35] while PVA was considered for its hydrophilic, semi-crystalline and cross-linkable nature, to achieve excellent membrane stabilities. Prepared PMPS membrane surface was modified by metal (copper) loading by ion-exchange process to improve the mono-valent ion selectivity of membrane, without any significant deterioration in membrane stability and transport properties. Modified membranes with controlled metal loading were characterized by several techniques in order to understand how the microstructure of this composite membrane affects its transport properties.

Methods

Materials

Poly(2-acrylamido-2-methyl-propane-sulfonic acid) (PMPS) (15% solution in water) was obtained from Sigma Aldrich Chemicals. Poly(vinyl alcohol) (PVA; MW, 125 000; degree of polymerization, 1700; degree of hydrolysis, 88%), hydrazine hydrate, EDTA, formaldehyde, H_2SO_4, $CuSO_4$, $NiCl_2$, $ZnCl_2$, NaCl and Na_2SO_4 (AR grade) were obtained from SD fine chemicals India, and used without any further purifications. In all experiment deionized water was used.

Preparation of PMPS membrane

Pristine PMPS membrane was prepared by solution casting method (Scheme 1). In a typical method, a known amount of PVA (8.0%, w/v) was dissolved in DI water at 80 ^{o}C under

stirred condition. Resultant solution was cooled to 30 ^{o}C and desired amount of PMPS (PVA and PMPS weight ratio was 1:2) was added. Resultant viscous solution was stirred thoroughly until a homogeneous colourless solution was obtained (6 h). Then homogeneous viscous solution was transformed into thin film onto a cleaned glass plate and dried at 60 ^{o}C in vacuum oven for 24 h. Flexible and transparent thin film was peeled off and cross-linked with formal solution ($HCHO+H_2SO_4$) for 3 h at 60 ^{o}C. The resulting membrane was washed thoroughly by DI water and conditioned in 0.1 M HCl and NaOH solutions, successively.

Metal (Cu) loading on PMPS membrane

Copper loading on the surface of PMPS membrane was achieved by ion-exchange method (electro-less plating) reported earlier.[36,37] The membrane was mounted at the bottom of the inner compartment in a two-compartment cell. $CuSO_4$ solution (0.1 M) and hydrazine hydrated solution (8%, v/v), were fed in the inner and outer compartment, respectively, for desired time. Constant stirring in inner compartment allowed exchange of Cu^{2+} with dissociated H^{+} from $–SO_3H$ groups (PMPS membrane matrix). Exchanged Cu^{2+} were further reduced in to metallic state (Cu) due to presence of hydrazine hydrate on the other side of the membrane. Different extent of metal loading density was achieved at different reaction time (1.0-3.0 h). It was observed maximum metal loading (metal coverage) was reached over the entire membrane surface at 3.0 h reaction time. Thus obtained metal loaded PMPS membranes were thoroughly washed with distilled water and equilibrated in 1 M NaCl for subsequent studies. Metal loaded PMPS membranes were designed as PMPS-X, where X denotes reaction time (h).

Instrumental analysis

Detailed instrumental analysis (FTIR, TGA, DSC, DMA and SEM) are included in the ESI Section S2.

Physicochemical and stabilities test of metal deposited membranes

Detailed procedures used for determination of water uptake and ion exchange capacity (IEC) are included in ESI section S2. Membrane stabilities were assessed under oxidative (Fenton's reagent) and hydrolytic environments.[38] Small pieces of membrane samples of known weight were soaked in Fenton's reagent (3% H_2O_2 containing 3 ppm $FeSO_4$) at 80 ^oC for 3 h. Membrane stability was assessed by deterioration in membrane weight. For the hydrolytic stability test, small piece of membrane was boiled in water for 24 h at 120 °C in a pressurized closed vial. Metal leaching out tests were also performed under hydrolytic conditions by recording metal loading density.

Electrochemical characterizations

Membrane conductivity for pristine and metal Cu loaded PMPS membranes was measured in equilibrium with different electrolytic environments (NaCl, $ZnCl_2$, and $NiCl_2$) of 0.1M concentration using potentiostat/galvanostat frequency response analyzer (Auto Lab, Model PGSTAT 30). Membranes were tightly sandwiched between two electrodes (circular stain less steel with 4 cm^2 area). Direct current (DC) and sinusoidal alternating currents (AC) were supplied between both electrodes to record frequency (10^6-1 Hz) at 1 μA/s scanning rate and resulting Nyquist plots were used to determine the resistance by Fit and Simulation method.[39]

Permselectivity for different ions across pristine PMPS and PMPS-3 membrane was estimated by counter-ion transport number in the membrane phase by membrane potential measurements. A two-compartment membrane cell (7.0 cm^2 effective membrane area) was used for membrane potential measurement.[40] Both compartments were fed with NaCl solutions of unequal concentrations and to minimize the effect of boundary layer condition, both the compartments were vigorously stirred. In equilibrium conditions, the potential aroused across the membrane was recorded by digital multimeter using saturated calomel electrodes and salt bridges. Counterion transport number in the membrane phase was

estimated by the TMS (Teorell, Meyer, and Sievers) approach.[40] Details for the determination of counterion transport number and membrane permselectivity are included in the ESI section S3.

The chronopotentiometric responses (described in ESI section S4) for metal loaded PMPS-3 membrane were recorded in equilibrium with different electrolyte solutions (NaCl, $NiCl_2$ and $ZnCl_2$) of 0.01 M.[41]

Electrodialysis experiments

To access the electrodialysis (ED) separation performance of prepared PMPS membranes for Na^+/Ni^{2+} and Na^+/Zn^{2+}, ED experiments were performed in a laboratory-scale unit (ESI Fig. S1). ED unit contained 4 cell pairs PMPS cation selective membrane and commercially sourced anion-exchange membrane (80 cm^2 effective area) (ASV supplied by Selemion, Japan). Properties of AEM are included in (ESI Table S1). Both types of membranes were alternatively arranged between the electrodes with help of membrane gasket and spacers. The flow pattern of the ED cell was based on parallel-cum-series. There was three compartments, electrodes wash (EW), dilute compartment (DC), and concentrated compartment (CC). The feed flow velocity of each stream was kept constant (0.006 m^3/h) using peristaltic pumps. Na_2SO_4 solution (0.10 M) was recirculated in both electrode wash (EW) compartments, separately. Initially, 500 cm^3 of mixed electrolyte solution [NaCl (3000 ppm) + MCl_2 (1000 ppm): M= Zn or Ni] was fed into the DC and deionized water was used into CC in recirculation mode. Precious metal oxide coated titanium sheets (TiO_2 sheet coated with a triple precious metal oxide (titanium-ruthenium-platinum), of 6.0 μm thickness, and 8.3×10^{-3} m^2 effective area) obtained from Titanium Tantalum Products (TITAN, Chennai, India) were used as the cathode and anode. A DC power supply (Aplab India, model L1285) was used to apply constant potential across the electrodes and variation in current was recorded as a function of time using a digital multimeter in series. Change in concentration of

Ni^{2+} or Zn^{2+} was determined by EDTA complexometry titration. The bivalent cation leakage (Ni^{2+} or Zn^{2+}) was calculated using following equation

$$Ni^{2+}/Zn^{2+}(\%) = \frac{\text{mass of } Ni^{2+}/Zn^{2+} \text{in concentrated cell}}{\text{mass of } Ni^{2+}/Zn^{2+} \text{ in concentrated cell and diluted cell}} \times 100 \qquad (1)$$

Results and discussion

Structural and morphological characterizations of membranes

PMPS membranes were prepared by solution casting method and characterized by FTIR (Fig. 1a). Presence of amide group in PMPS was confirmed by absorption band at 1556 and 1650 cm^{-1}.[42] Strong band at 1039 cm^{-1} was attributed to S=O stretching (–SO_3H).[43] The absorption band at 1168 cm^{-1} attribute to the C–O–C stretching vibration.[44] The broad band at 3435 cm^{-1} arouse due to presence of –OH groups. In addition, almost all the characteristic peak of PMPS was present in the spectrum PMPS-3 (Fig. 1b). SEM image of pristine PMPS membrane showed homogeneous and dense in nature without any holes, cracks and phase separation (Fig. 2a). While, membrane surface roughness increased with Cu loading in the matrix (PMPS-3) Fig. 2b. SEM image clearly demonstrate homogeneous metal deposition in the membrane matrix. Optical images revealed white colour of pristine PMPS membrane progressively turned Cu metallic coloured with Cu loading in the matrix (Fig. 2c-f). SEM-EDX study conformed Cu loading in PMPS-3 membrane matrix Fig. 2g.

Thermal, mechanical and chemical stabilities

Thermal degradation for pristine PMPS and Cu loaded PMPS membranes were studied by TGA curves (Fig. 3). First step weight loss (below 100 ^oC) was attributed to the loss of absorbed water in membrane voids/pores. In second step, (100-250 ^oC) weight loss was observed due to loss in bound water. Weight loss in third step (400-450 ^oC) was attributed to the decomposition of functional group and polymer membrane matrix. Although, weight loss (%) of all membranes are broadly similar, but careful observation revealed that weight loss

(%) for PMPS-3 membrane was minutely less in compare with pristine PMPS membrane, may be due to 7.3 mg/cm^2 Cu loading density of the PMPS-3 matrix. This may be attributed to the coverage of polymer matrix by metal particles. DSC thermogram for pristine PMPS membrane showed endothermic peak at 120 ^{o}C (ESI Fig. S2). After Cu loading endothermic peak values was progressively increased and PMPS-3 membrane showed quite higher T_g value (130 ^{o}C). Positive shift in T_g value after Cu loading in the membrane matrix may be aroused due to enhanced compactness and stiffness of the polymer matrix.

Mechanical stability of the membranes was investigated by dynamic mechanical analysis (DMA) ESI Fig. S3. Mechanical stability of pristine PMPS membrane (~1800 MPa storage modulus) was significantly improved with metal loading in the membrane matrix, and PMPS-3 membrane exhibited ~4300 MPa storage modulus. Similar observation was also obtained from burst strength data. Improved mechanical stability metal loaded PMPS membrane was further attributed to the increased compactness, stiffness and strong interaction between metal and polymer matrix.

The oxidative and hydrolytic stabilities of prepared membranes were assessed in term of weight loss. Pristine PMPS/PVA membrane showed 7.95% weight loss in compare with 3.25% weight loss for PMPS-3 membrane under strong oxidative conditions (Table 1). Improved oxidative stability for metal loaded PMPS membrane was attributed the presence metal particles in the membrane matrix reduced the chemical degradation of polymer matrix. Hydrolytic stability of an ion-exchange membrane is one of the essential features and plays an important role for membrane applications. Hydrolytic test of developed membrane was also examined by weight loss and metal loaded PMPS membrane exhibited reduced hydrolytic weight loss (4.75% for PMPS-3 membrane) in compare with pristine PMPS membrane (7.50%) Table 1. Thus, loading Cu in the PMPS membrane matrix improved thermal, mechanical, oxidative and hydrolytic stabilities.

Physicochemical properties of membranes

Membrane thicknesses were varied between 150-165 μm ± 5 μm. Membrane water uptake (WU) value throws the light on hydrophilic nature, presence of pores/cavities in the membrane matrix and dimensional properties. WU for pristine PMPS membrane (45.55%) was significantly reduced with Cu loading in the membrane matrix and PMPS-3 membrane showed 17.26% WU (Table 2). Generally, membrane absorbs water due to the presence of functional groups and thus hydrogen bonding. Metal particles occupy the interstitial position in functional groups and cavities and lowered the WU values. In addition, metal loading also altered the membrane hydrophilic nature and as reference and as result PMPS-3 membrane showed 72^{o} contact angle in compare with 55^{o} for pristine PMPS membrane. Reduced hydrophilic nature of Cu loaded PMPS membrane may be explained by coverage charged functional groups ($–SO_3H$) by metal particles in membrane matrix. Idea about exchangeable charged groups in membrane matrix may be obtained by ion-exchange capacity (IEC) value.

To assess the ionic charged nature of the membrane in terms of equivalent of ionic functional groups present in the per unit dry weight, IEC is a necessary parameter, which also reveals ion-conductive nature of the membrane. Metal loaded membrane exhibited 1.08-1.40 meq/g IEC value in compare with pristine PMPS membrane (1.48 meq/g) Table 2. Lowered IEC values for metal loaded PMPS membrane may be attributed to reduced density of ionic sites available for ion-exchange. Here it is important to record that Cu^{+2} were exchange by H^{+} present in the membrane matrix and reduced with hydrazine hydrate. This phenomenon accompanied by lowering in exchangeable ion-sites by coverage with metal particles.

Electrochemical properties of membranes

Membrane conductivity in equilibration with 0.10M electrolyte solutions (NaCl, $NiCl_2$ and $ZnCl_2$) for different membranes has been included in Fig. 4. Conductivity of pristine PMPS membrane 30.0 mS cm^{-1} (at 30^{o}C in equilibration with 0.10 M NaCl solution) was reduced to

17.2 mS cm^{-1} for PMPS-3 membrane may be due to coverage of charged functional groups by Cu particles in the membrane surface. It seems, metal deposition on the membrane surface partially blocked the ionic cluster by lowering the number ion-exchange sites responsible for ion conduction.[19] In addition, low ionic conductivity for metal loaded PMPS membrane may be attributed to: (i) less availability of water in the membrane matrix (low WU) necessary for ionic conduction; (ii) IEC and/or (iii) interaction between PMPS membrane matrix and metal particles. All these above-mentioned reasons seem to be responsible for the observed low membrane conductivity for Cu loaded PMPS membrane.

Activation energy (E_a) is the minimum energy required for ion conduction, and low activation energy responsible for minimum energy loss during ionic transportation due to resistance caused by membrane matrix. At different temperature, ion conductivity values were used with advantages for the estimation of E_a by Arrhenius plots using following equation.

$$E_a = -b \times R \quad (2)$$

Where E_a is the activation energy (kJ/mol), R the universal gas constant ($R = 8.314 \mathrm{J/(mol\ K)}$, and b the slope of linear regression of $\ln \boldsymbol{\kappa}^m$ versus $1000/T$ plots (Fig. 4). The temperature (30-90 ^oC) dependent conductivity for pristine and metal loaded PMPS membranes showed consistency with the Arrhenius relationship. Loading of Cu particle in the membrane matrix increased the activation energy values Table 2. As a reference, activation energy for pristine PMPS membrane (8.31 kJ mol^{-1}) is lower in compare with PMPS-3 membrane (10.10 kJ mol^{-1}). Similar trend was observed in case of temperature dependence conductivity of PMPS-3 membrane in equilibration with NaCl, $NiCl_2$ or $ZnCl_2$ solutions (Fig. 4b). Further, high conductivity of PMPS-3 membrane under experimental conditions confirmed their suitability for electrochemical applications.

The permselectivity arises due to the nature of the membrane for discrimination between counter-ions and co-ions. This type of discrimination arises because of the nature and magnitude of the charge on the membrane matrix. IEC values revealed moderately reduction exchangeable charge concentration after metal loading in the membrane matrix. This seems to be quite reasonable in the light of the preceding discussion. Counter-ion transport number in the membrane phase measurements were performed to investigate the alteration in permselectivity (*P*s) for different counter-ions (Na^+, Ni^{2+}, and Zn^{2+}) with metal loading in the PMPS membrane matrix. In spite higher Stokes radius of Zn^{2+} in compare with Ni^{2+}, P_s values for Ni^{2+} across pristine and metal loaded PMPS are marginally smaller than Zn^{2+}. This may be attributed to relatively low dissociation of $NiCl_2$ in compare with $ZnCl_2$ under similar concentration range. Another interesting point is how Cu loading in the membrane matrix affects the permeselctivity for Na^+, Ni^{2+} and Zn^{2+} counter-ions. Deterioration in *Ps* for Na^+ after metal loading (PMPS-3 membrane) in compare with pristine PMPS membrane was about negligible (3.7%), while P_s for Ni^{2+} and Zn^{2+} declined about 29.7% and 28.5%, respectively (Fig. 5). Results suggest that Cu loaded membrane (especially PMPS-3) exhibited blocking behaviour, which further increased with metal loading density. Cu metal particles occupy the space in ionic clusters and interrupt the ion conducting path thus transport properties. Furthermore, Stokes radius of the hydrated counter-ions also plays important role for their transport across the membrane, which varies as: Na^+ (3.6 Å) < Ni^{2+} (4.0 Å) < Zn^{2+} (4.3 Å).[45] The membrane modification with metal particle seems to improve its blocking behaviour for the transport of bi-valent metal cations (Ni^{2+}, and Zn^{2+}), because after metal loading selectivity of membrane drops significantly, which will reduce metal leakage during electrodialysis. However, deterioration in Ni^{2+}/Zn^{2+}, accompanied with loss in membrane ionic conductivity and in fact ion conductivity decreased in proportional to metal loading density in the membrane matrix.

Chronopotentiometric response of membrane

Detailed description of membrane chronopotentiometry analysis has been included in (ESI S4 section). The chronopotentiometric responses for PMPS-3 membrane in equilibrium with NaCl, $NiCl_2$ and $ZnCl_2$ solution (0.01 M solution) were recorded at 2.0 mA cm^{-2} applied current density and included in Fig. 6. PMPS-3 membrane showed well defined chronopotentiometric inflection with 4.00, 6.32, and 6.92 mA s cm^{-1} $I\tau^{1/2}$ (I: applied current density and τ: transition time) values in equilibration with NaCl, $NiCl_2$ and $ZnCl_2$ solution (0.01 M). It was also observed the $I\tau^{1/2}$ values were fairly constant and independent of I at a given concentration of electrolyte. In chronopotentiograms, inflection aroused due to concentration polarization at membrane interface under applied current, and comparatively low $I\tau^{1/2}$ values in equilibrium with NaCl solution confirmed rapid polarization of membrane interface because of easy transport and high mobility of Na^+. Interfacial character, polymer nature and external electrolytic environment govern ion selectivity and transport property of membrane. Because of delayed inflection in chronopotentiograms (Fig. 6), electro-migration of Ni^{2+}/Zn^{2+} across PMPS-3 membrane was slower in compare with Na^+. This was attributed to the negligible transport (leakage) of Ni^{2+}/Zn^{2+} under electrodialytic conditions across PMPS-3 membrane.

Electrodialysis experiment

The i–V curves for pristine and metal particles loaded PMPS membrane showed three typical characteristic regions viz. Ohmic, non-Ohmic, and plateau length, in equilibration with 0.1 M NaCl solution Fig. 7. Obtained results confirmed ion transport and concentration polarization phenomenon under the operating conditions across these membranes. Pristine PMPS membrane exhibited relatively high ΔV and Δi values, because of fast electro-transport of counter-ions from diffusive boundary layer to membrane matrix and low membrane resistance (Fig. 4A). Further, these values decreased with metal loading in the membrane

matrix. This may be attributed to the deterioration in conductivity with metal loading in the membrane matrix, which partially reduced the transport properties and induced mono- or bi-valent ion selectivity.

To block the transport (leakage) of bi-valent ions (Ni^{2+}/Zn^{2+}) by metal (Cu) modification of PMPS membrane and efficient electrolytic separation of Na^+ in aqueous media is main objective of the resent work. Electrodialysis experiments were performed in a cell containing 4 cell pairs of PMPS and anion-exchange membrane, to asses evaluate the blocking behaviour of metal loaded membranes for bi-valent cations in presence of mono-valent cation (Na^+). Series of electrodialysis experiments for the separation of Na^+ and Ni^{2+}/Zn^{2+} were performed at constant applied voltage (4.0 V) under passage of about 400 A s current. Mixed electrolyte solutions [NaCl (3000 ppm) + $NiCl_2$ or $ZnCl_2$ (1000 ppm)] were recirculated as initial feed of DC, while deionized water was used as feed in CC. Both electrode compartments were recirculated with Na_2SO_4 solution (0.1 M), to avoid any undesired electrode reactions. Electrodialytic flux data for Na^+, Ni^{2+} and Zn^{2+} under similar experimental conditions across pristine and Cu loaded membranes are included in Table 3 (detailed method for the estimation of ionic flux data is included in ESI Section S5). In case of pristine PMPS membrane, Na^+ flux was very high (about 30 times) in compare with Ni^{2+}/Zn^{2+} flux (Table 3). Metal loading in PMPS membrane matrix was responsible for significant reduction in flux for Ni^{2+}/Zn^{2+} without any deterioration in Na^+ flux. As reference, PMPS-3 membrane showed 29.13×10^{-7} mol m^{-2} s^{-1} flux for Na^+ in compare with extremely low flux for Ni^{2+}/Zn^{2+} (0.26×10^{-7} mol m^{-2} s^{-1} and 0.21×10^{-7} mol m^{-2} s^{-1}), respectively. Further flux ratio between Na^+ and Ni^{2+}/Zn^{2+} was significantly increased and found to be ~100, in case of electrodialytic separation using PMPS-3 membrane. Metal loaded membranes exhibited high Na^+ selectivity and impervious nature for Ni^{2+}/Zn^{2+} transport (Table 3). After metal loading, Ni^{2+}/Zn^{2+} leakage significantly dropped to 2.6 and 3.7% respectively across

PMPS-3 membrane, due to pore blockage by Cu metal particles. Metal modification of PMPS matrix certainly affect the membrane microstructure, and Cu particles believed to accommodate within hydrophilic ionic clusters (transport properties of pristine PMPS membrane also partially reduced with metal loading). Metal loading in the PMPS significantly reduced transport (leakage) bi-valent metal ions (Ni^{2+}/Zn^{2+}) without any significant deterioration in transport properties for Na^{+}, may be due to partial blocking behaviour of metal particles. Metal (Cu) loading in the PMPS matrix was achieved by ion-exchange process and thin uniform metal layer is required on the surface of cation-exchange membrane to allow fast passage of small ion (Na^{+}) and blockage of relatively bigger ions. However, partial decrease in membrane conductivity with metal loading significantly reduced Ni^{2+}/Zn^{2+} leakage, seems to be insignificant to reduce the electrodialytic performance of metal loaded membranes.

Energy consumption (W, kWh/kg of salt recovered) and current efficiency (CE) values are important parameter to assess the suitability of the membrane. Energy consumption and *CE* (%) data during electrodialysis using pristine and metal loaded PMPS membranes under similar conditions are included in Table 3. With metal loading, *W* values were partial increased, while CE decreased, may be due to reduction in membrane conductivity. Metal loading in the membrane matrix was achieved by ion-exchange process through exchangeable $–SO_3H$ groups and responsible for slight reduction in membrane charged nature. Metal loading in the membrane matrix forma thin rigid layer and certainly affect the microstructure of the membrane thus, ionic transport was partially inhibited. On the other hand, the surface compactness of membranes was enhanced, and easy accessibility of bulkier counter-ions to the fixed ionogenic sites on the membrane matrix became more and more difficult for more compact/rigid membrane matrix and difficult to transport through the membrane. Furthermore, electrodialytic performance parameters (*W* and *CE*) also depend on

the operating conditions of an ED unit. Under optimum operating conditions (after the passage of 400 A s electricity), for PMPS-3 membrane, *CE* and *W* were found to be 73.4% and 0.97 kWh kg^{-1}, respectively, which showed the potential of the developed AEM for electrochemical devices.

In Table 4, IEC and Zn^{2+} leakage of under electrodialytic conditions across PMPS-3 membrane was compared with state-of-the-art cation exchange membranes reported in the literature.[7,18,19,46] Generally, polyaniline or polyquaternium-7 modification on Nafion 117 or JAM-II-10 commercial membranes marginally reduced the membrane IEC values (as observed Cu modification in this case). It was also observed that modified state-of-the-art CEMs showed relatively low Zn^{2+} leakage in compare with corresponding unmodified CEMs. Apart from extremely low Zn^{2+} leakage for reported PMPS-3 membrane (2.6%) in compare with state-of-the-art CEMs (unmodified and modified) showed excellent selectivity of previous one for transport of Na^{+} in presence of Zn^{2+} or Ni^{2+}. Thus, PMPS-3 membrane showed excellent pore-size sieving effect and blocked pore/channels with metal (Cu) loading effectively prevent the transport of Zn^{2+} or Ni^{2+} without any significant deterioration in Na^{+} transport. These findings demonstrate a versatile route for fine tuning between permselectivity and ionic flux across the CEM.

Conclusions

PMPS membrane was prepared and controlled metal (Cu) loading was achieved by ion-exchange process on the surface of cation exchange membrane to improve the monovalent selectivity of the membrane. The controlled metal loading was achieved in single-step, where metallic counter-ion (Cu^{2+}) and reducing agent (hydrazine hydrate) diffuse through both sides of the membrane matrix, led to the formation of homogenous and thin metallic layer as confirmed by SEM, EDX and contact angle studies. Metal loading in the PMPS cation-exchange matrix didn't significantly alter the membrane stability, but membrane transport

properties and conductivity were partially reduced. Blocking behaviour of metal loaded membranes increased with metal loading density. It was believed that metal particles (Cu) occupied the space in ionic clusters and interrupt the ion conducting path thus transport properties. Loaded metal particles significantly reduced the transport (leakage) of bi-valent metal cations (Ni^{2+} and Zn^{2+}), without any significant deterioration in transport of Na^{+} during electrodialysis. Further, extremely low Zn^{2+} leakage for PMPS-3 membrane in compare with other state-of-the-art CEM was attributed to excellent pore-size sieving effect. This work could contribute the understanding of controlled transport behaviour of mono- and bi-valent ions for their electrodialytic separation. Further, loading metal in the thin film matrix by ion-exchange process can be considered as valuable tool for the advancement of developing polymer-metal composite for diversified electrochemical applications.

Acknowledgements

CSIR-CSMCRI registration no.: 110/2015. This work is supported by Department of Science and Technology, New Delhi (Project no. SR/S1/PC-62/2012), Govt. of India. Instrumental support received from Analytical Science Division, CSMCRI is also gratefully acknowledged.

References

1 H. Dong, L. Zhao, L. Zhang, H. Chen, C. Gao and W. S. W. Ho, *J. Membr. Sci*., 2015, **476**, 373–383.

2 S. M. Hosseni, M. Nemati, F. Jeddi, E. Salehi, A. R. Khodabakhshi and S. S. Madaeni, *Deaslination*, 2015, **359,** 167-175.

3 T. Xu, *J. Membr*. *Sci*., 2005, **263,** 1–29.

4 Y. Gong, L. M. Dai, X. L. Wang and L. X. Yu, *Desalination*, 2006, **191,** 193–199.

5 Ch. Klaysom, R. Marschall, S. H. Moon, B. P. Ladewig, G. Q. M. Lu and L. Wang, *J. Mater*. *Chem*., 2011, **21,** 7401–7409.

6 A. K. Thakur, N. Srivastava, T. Chakrabarty, B. Rebary, R. Patidar, R. J. Sanghavi, V. K. Shahi and P. K. Ghosh, *Desalination*, 2014, **335,** 96–101.

7 G. Chamoulaud and D. Belanger, *Langmuir*, 2004, **20,** 4989–4995.

8 B. M. Asquith, J. Meier-Haack, C. Vogel, W. Butwilowski and B.P. Ladewig, *Desalination*, 2013, **324,** 93–98.

9 H. Farrokhzad, T. Kikhavani, F. Monnaie, S. N. Ashrafizadeh, G. Koeckelberghs, T. Van Gerven and B. Van der Bruggen, *J. Membr. Sci.*, 2015, **474,** 167–174.

10 X. Q. Cheng, L. Shao and C. H. Lau, *J. Membr. Sci.*, 2015, **476,** 95–104.

11 J. Yin and B. Deng, *J. Membr. Sci*., 2015, **479,** 256–275.

12 M. Taky, G. Pourcelly and A. Elmidaoui, *Hydrometallurgy*, 1996, **43,** 63–78.

13 M. Boucher, N. Turcotte, V. Guillemette, G. Lantagne, A. Chapotot, G. Pourcelly, R. Sandeaux and C. Gavach, *Hydrometallurgy*, 1997, **45,** 137–160.

14 L. X. Tuan, C. Buess-Herman and H. D. Hurwitz, *J. Membr. Sci*., 2008, **323,** 288–298.

15 S. M. Hosseini, S. S. Madaeni, A. R. Khodabakhshi and A. Zendehnam, *J. Membr. Sci*., 2010, **365,** 438–446.

16 R. K. Nagarle, G. S. Gohil, V. K. Shahi, G. S. Trivedi and R. Rangarajan, *J. Colloid Interface Sci*., 2004, **277,** 162–171.

17 A. Razmjou, J. Mansouri and V. Chen, *J. Membr. Sci*., 2011, **378,** 73–84.

18 S. Tan, A. Laforgue and D. Belanger, *Langmuir*, 2003, **19,** 744–751.

19 S. Tan and D. Belanger, *J. Phys. Chem. B*, 2005, **109,** 23480–23490.

20 X. T. Le, P. Viel, P. Jegou, A. Garcia, T. Berthelot, T. H. Bui and S. Palacin, *J. Mater. Chem*., 2010, **20,** 3750–3757.

21 T. Sata, Y. Ishii, K. Kawamura and K. J. Matsusaki, *Electrochem. Soc*., 1999, **146,** 585–591.

22 R. K. Nagarale, G. S. Gohil and V. K. Shahi, *J. Membr. Sci*., 2006, **280,** 389–396.

23 T. Sata, T. Funakoshi and K. Akai, *Macromolecules*, 1996, **29,** 4029–4035.

24 G. S. Gohil, V. V. Binsu and V. K. Shahi, *J. Membr. Sci*., 2006, **280,** 210–218.

25 Y. Hu, M. Wang, D. Wang, X. Gao and C. J. Gao, *J. Membr. Sci*., 2008, **319,** 5–8.

26 V. Vatanpour, S. S. Madaeni, A. R. Khataee, E. Salehi, S. Zinadini and H. A. Monfared, *Desalination*, 2012, **292,** 19–29.

27 A. Razmjou, E. Arifin, G. Dong, J. Mansouri and V. Chen, *J. Membr. Sci*., 2012, **415,** 850–863.

28 T. Sata, R. Izuo and K. Takata, *J. Membr. Sci*., 1989, **45,** 197–208.

29 T. Sata and R. Izuo, *J. Appl. Polym. Sci*., 1990, **41,** 2349–2362.

30 K. Takata, Y. Yamamoto and T. Sata, *J. Membr. Sci*., 2000, **179,** 101–107.

31 M. Kumar, B. P. Tripathi and V. K. Shahi, *J. Membr. Sci*., 2009, **340,** 52–61.

32 S. Abdu, M-C. Manuel-Cesar, J. E. Wong, M. Garcia-Gabaldoon and M. Wessling, *ACS Appl. Mater. Interfaces*, 2014, **6,** 1843−1854.

33 L. Ge, L. Wu, B. Wu, G. Wang and T. Xu, *J. Membr. Sci*., 2014, **459,** 217–222.

34 L. Ge, X. Liu, G. Wang, B. Wu, L. Wu, E. Bakangura and T. Xu, *J. Membr. Sci*., 2015, **475,** 273–280.

35 H. Pei, L. Hong and J. Y. Lee, *J. Power Sources*, 2006, **160,** 949–956.

36 C. Yi-Lin and C. Tse-Chuan, *J. Electroanal. Chem*., 1993, **360,** 247–259.

37 V. K. Shahi, R. Prakash, G. Ramachandraiah, R. Rangarajan and D. Vasudevan, *J. Colloid and Interface Sci*., 1999, **216,** 179–184.

38 B. P. Tripathi, T. Chakrabarty and V. K. Shahi, *J. Mater. Chem*., 2010, **20,** 8036–8044.

39 M. Kumar, S. Singh and V. K. Shahi, *J. Phys. Chem*. *B*, 2010, **114***,* 198–206.

40 R. K. Nagarale, G. S. Gohil, V. K. Shahi and R. Rangarajan, *J. Colloid Interface Sci*., 2005, **287,** 198–206.

41 V. K. Shahi, S. K. Thampy and R. Rangarajan, *J. Membr. Sci*., 2002, **203,** 43–51.

42 J. Qiao, T. Hamaya and T. Okada, *Chem. Mater*., 2005, **17,** 2413–2421.

43 J. Qiao, T. Hamaya and T. Okada, *J. Mater. Chem*., 2005, **15,** 4414–4423.

44 T. Chakrabarty, B. Shah, N. Srivastava, V. K. Shahi and U. Chudasama, *J. Membr. Sci*., 2013, **428,** 462–469.

45 H. Ashjian, E. Brunswick, Q. N. Le, C. Hill, D.O. Marler, J. Shim and S. S. Wong, Naphthalene Alkylation Process. US Patent Number 3035563, 1991.

46 J. Li, M-l. Zhou, J-y. Lin, W-y Ye, Y-q. Xu, J-n. Shen, C-j. Gao, B. Van der Bruggen, *J. Membr. Sci*., 2015, **486,** 89–96.

Table 1 Oxidative and hydrolytic weight loss for different membranes.

Membrane	W_{OX}(wt %)*	W_{HS}(wt %)*
PMPS	7.95	**7**.50
PMPS-1	6.25	7.11
PMPS-2	4.32	5.15
PMPS-3	3.25	4.75

**During estimation of W_{ox} and W_{HS} (%) weight loss, weight of Cu deposited on different membranes was reduced from total membrane weight for initial and after oxidative or hydrolytic treatment.*

Table 2 Water uptake (WU), ion-exchange capacity (IEC), contact angle (θ), metal loading (mg/cm^2) and burst strength data for different membranes

Membrane	Metal loading (mg/cm^2)	WU (%)	IEC (mequiv g^{-1})	Contact angle (θ)	Burst strength ($kg\ cm^{-2}$)	E_a ($kJ\ mol^{-1}$)
PMPS	-	45.55	1.48	50	3.16	8.31
PMPS-1	1.5	27.72	1.40	56	3.24	9.08
PMPS-2	4.5	22.65	1.18	65	3.32	9.55
PMPS-3	7.3	17.26	1.08	72	3.45	10.10

Table 3 Electrodialysis separation performance of mixed electrolyte solutions [NaCl (3000 ppm) + $NiCl_2$ or $ZnCl_2$ (1000 ppm)] for pristine PMPS and Cu loaded PMPS membrane at 1.5 V/cell pair applied potential: applied coulombs = 400 As (feed for permeate stream: distilled water)

Membranes	Flux of different counter-ions $\times 10^{-7}$ (mol m^{-2} s^{-1})			Leakage of different ion (%)		Current efficiency (%)	Energy consumption (kWhr/kg of salt removed
	Na^+	Ni^{2+}	Zn^{2+}	Ni^{2+}	Zn^{2+}		
PMPS	34.81	1.23	1.17	9.6	8.2	78.6	0.88
PMPS-1	32.67	0.64	0.57	5.8	4.5	75.4	0.92
PMPS-2	30.76	0.48	0.37	4.1	3.9	74.8	0.93
PMPS-3	29.13	0.26	0.21	3.7	2.6	73.4	0.97

Table 4 Comparison of IEC and Zn^{2+} leakage under electrodialytic conditions of PMPS-3 and reported CEM in literature.

Membranes	IEC (mequiv. g^{-1})	Zn^{2+} leakage (%)	Ref.
Nafion 117[a]	0.93±0.04	11±0.5	19
Naf P1-1-1[b]	0.78±0.04	5±0.5	19
CMX[c]	1.64±0.2	10.1	7&18
CSO[d]	1.04	9.1	46
JAM-II-10[e]	1.8-2.0	22.0	46
JAM-II-10 modified by polyquaternium-7	1.73	14.2	46
PMPS-3	1.08	2.6	In this manuscript

[a]Nafion 117: Perfluorosulphonic acid CEM supplied by DuPont.
[b]Naf P1-1-1: Polyaniline modified Nafion 117 composite membrane.
[c]CMX: Commercial CEM, NEOSEPTA CMX, produced by Tokuyama Corp.
[d]CSO: Commercial monovalent selective CEM supplied by Asahi (Japan).
[e]JAM-II-10: CEM supplied by Beijing Tingrun Membrane Technology Development company.

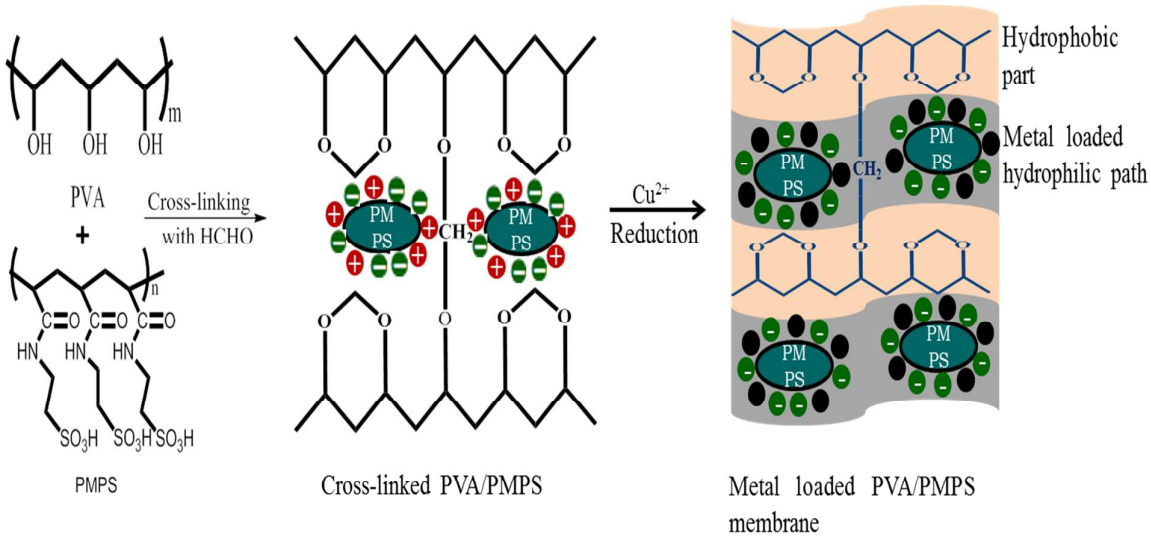

Scheme 1. Preparation of metal loaded PMPS membrane.

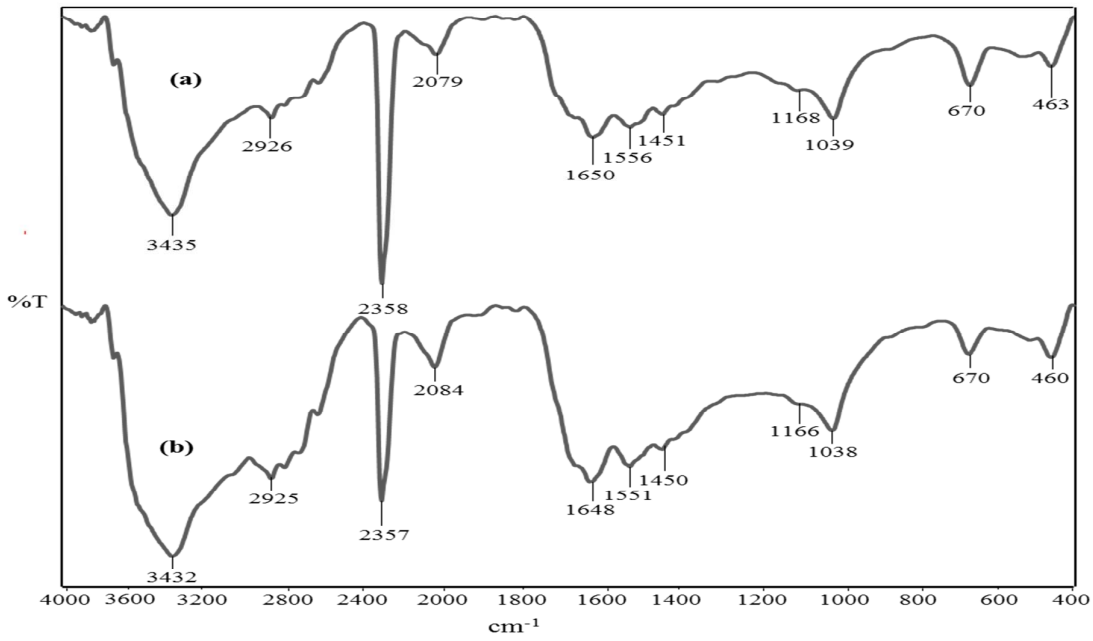

Fig. 1. FTIR spectra of (a) PMPS and (b) PMPS-3 membrane.

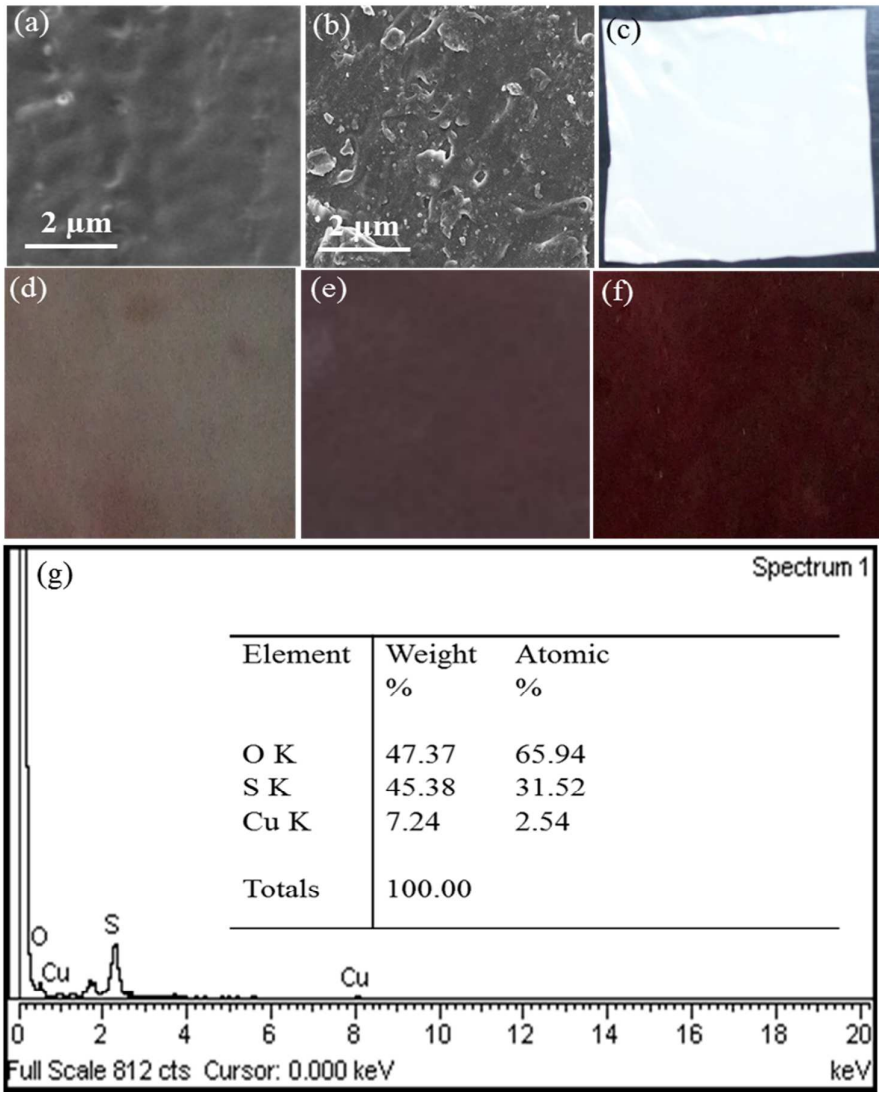

Fig. 2. SEM images for: (a) pristine PMPS membrane; and (b) metal loaded PMPS-3 membrane. Optical images for: (c) pristine PMPS; (d) PMPS-1; (e) PMPS-2 and (f) PMPS-3 membranes, and (g) EDX analysis of PMPS-3 membrane.

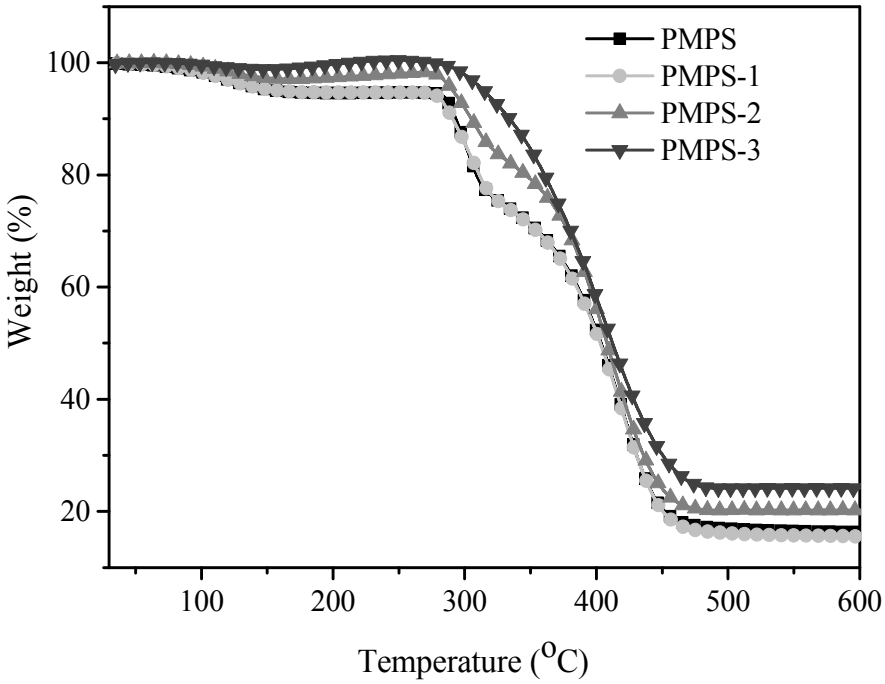

Fig. 3. TGA curves for different membranes.

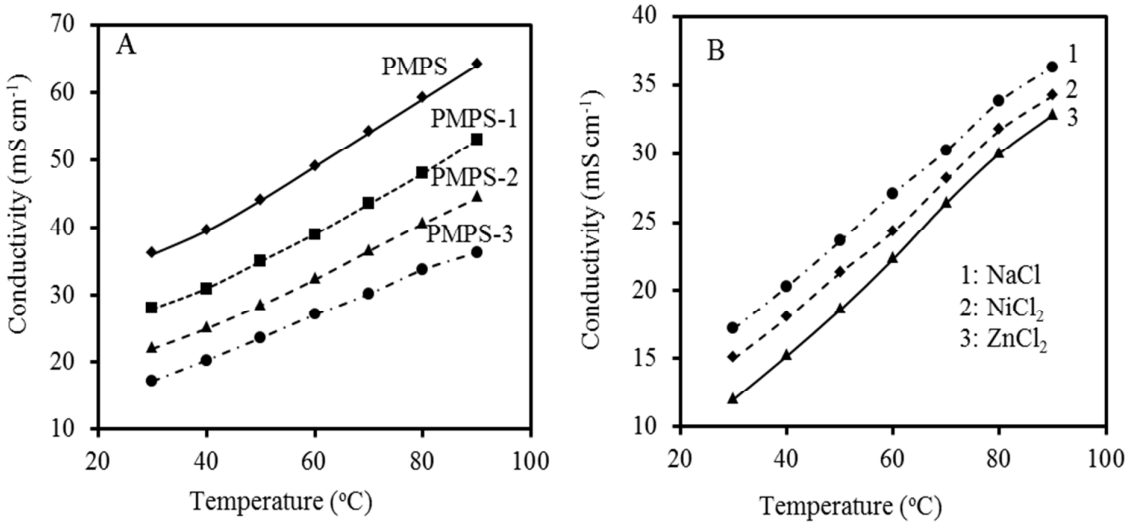

Fig. 4. The variation of conductivity for: (a) pristine PMPS and different metal loaded PMPS membranes in equilibration with NaCl (0.10 M) solution; (b) PMPS-3 membrane in equilibration with different electrolyte solutions (0.10 M).

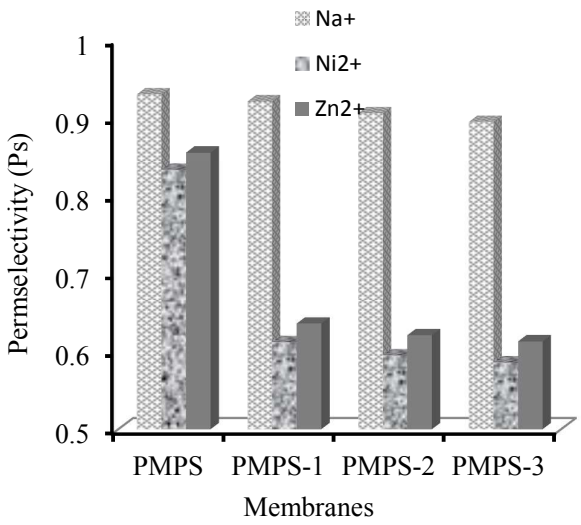

Fig. 5. Permselectivity of pristine PMPS and different Cu loaded membrane for different counter-ions (estimated from counter-ion transport number in membrane phase). Measuring error for permselectivity was 0.01.

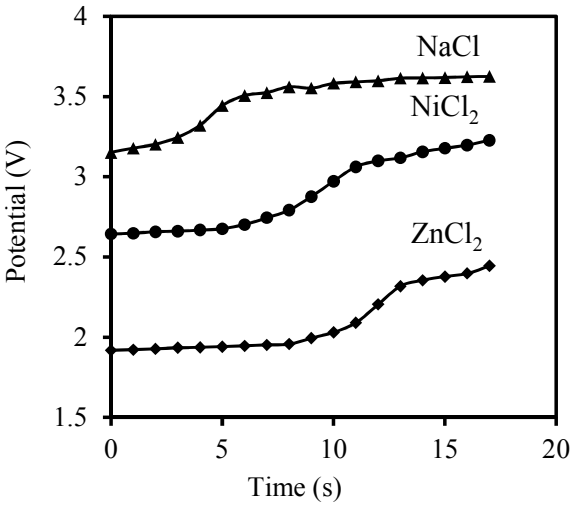

Fig. 6. Chronopotentiometric response for PMPS-3 membrane in equilibration with different electrolyte solution (0.01 M) at 2.0 mA cm^{-2} applied current density.

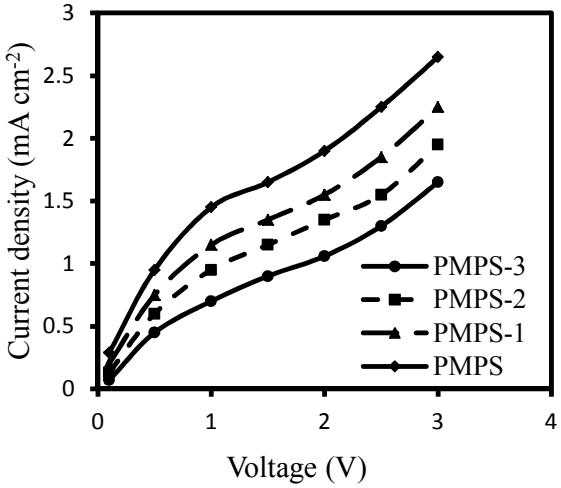

Fig. 7. Current-voltage (i-*v*) curves for pristine and metal loaded PMPS membranes in equilibration with NaCl solution (0.10 M).

Graphical absract